ANTENNA CIRCUIT MODEL
FOR TIME-DOMAIN TRANSIENT ANALYSIS

J. Bernardes, F. Peterkin, B. Hankla, J. Latess
Naval Surface Warfare Center, Dahlgren Division
Dahlgren, VA 22448

Abstract

When pulse-generating circuits excite antennas, the antenna often plays a major role in determining the characteristics of the radiated signal. Defining an equivalent electrical circuit for the antenna allows the simulation of the antenna's transient behavior. This type of simulation, carried out with circuit analysis software, generates time-domain currents at different points on the antenna structure. From these currents, the time-domain radiated electric field can be calculated.

This paper describes a procedure for developing a distributed RLC circuit model for a monopole antenna above a ground plane. The results from the modeling are compared to measurements of antenna current and radiated electric field.

I. INTRODUCTION

Various puled-power applications require predicting the transient behavior of antennas driven by pulse-generating circuits. A method is presented which models antenna transient behavior with a distributed-element circuit. This type of antenna model can predict antenna distributed currents when it is driven by circuits of arbitrary design. Parameter analysis and optimization is greatly simplified by the ability to simulate source-antenna interaction in a single circuit model.

This paper focuses on the circuit modeling of a particular type antenna, a monopole above a ground plane. A circuit model is developed for this antenna and its step-excitation currents are calculated. A radiation model predicts the radiated transient electric field based on the calculated currents. The chosen antenna geometry was implemented in a test setup. Current and field measurements from this setup are compared to the calculated currents and fields.

II. CIRCUIT-MODEL CONSTRUCTION

As shown in Fig. 1, the monopole antenna consists of a 20.3-cm diameter, 115.6-cm long, aluminum tube with a hemispherical cap at the lower end. This tube structure is elevated 3.8-cm above a ground plane. As illustrated in Fig. 1, the antenna is modeled as a distributed resistance-inductance-capacitance (RLC) circuit, analogous to a

transmission-line circuit model. The antenna tube is divided into a series of equal-length sections. A capacitance, an inductance, and a resistance form a circuit stage that represent each of the sections. The distributed capacitance and inductance sets propagation times of electrical transients on the antenna. The resistance determines the rate-of-damping of the induced transients. Capacitance is defined by the geometry of the antenna tube in relation to the ground plane. The inductance, also defined by geometry, is the self-inductance of the tube. The resistance is obtained from measurements.
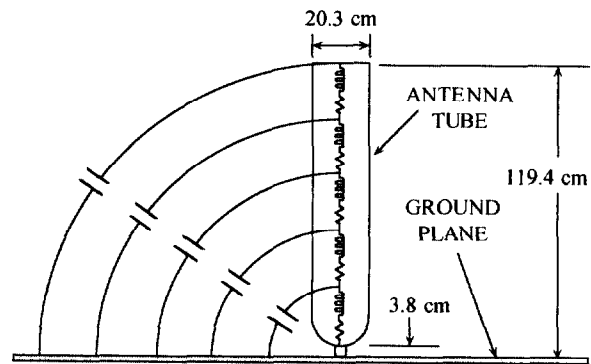

Figure 1. Monopole antenna with an illustration of its circuit model.

Distributed capacitance was calculated with the aid of Quickfield, an electrostatic field-mapping software. The antenna geometry is specified in Quickfield as a series of closely spaced but electrically isolated tube sections above a ground plane. A charge is applied to each section, and the electric potentials developed between the sections and the ground plane are calculated. The section capacitance is obtained from the ratio of the applied charge to the developed potential (C=Q/V).

An approximate equation for the inductance of a tube [1] was used to calculate the total self-inductance of the antenna tube. This inductance is divided equally among the stages of the antenna circuit model.

The resistance represents antenna radiation losses. Its placement in series with the tube inductance is guided by fact that radiation is caused by charge acceleration on the tube, which is also responsible for the inductance. The resistance is distributed equally among the stages of the circuit model, and its value was adjusted until the rate of decay of the oscillating antenna current matched measurements.

Report Documentation Page

Public reporting burden for the collection of information is estimated to average 1 hour per response, including the time for reviewing instructions, searching existing data sources, gathering and maintaining the data needed, and completing and reviewing the collection of information. Send comments regarding this burden estimate or any other aspect of this collection of information, including suggestions for reducing this burden, to Washington Headquarters Services, Directorate for Information Operations and Reports, 1215 Jefferson Davis Highway, Suite 1204, Arlington VA 22202-4302. Respondents should be aware that notwithstanding any other provision of law, no person shall be subject to a penalty for failing to comply with a collection of information if it does not display a currently valid OMB control number.

1. REPORT DATE	2. REPORT TYPE	3. DATES COVERED
JUN 1999	**N/A**	**-**

4. TITLE AND SUBTITLE	5a. CONTRACT NUMBER
Antenna Circuit Model For Time-Domain Transient Analysis	5b. GRANT NUMBER
	5c. PROGRAM ELEMENT NUMBER

6. AUTHOR(S)	5d. PROJECT NUMBER
	5e. TASK NUMBER
	5f. WORK UNIT NUMBER

7. PERFORMING ORGANIZATION NAME(S) AND ADDRESS(ES)	8. PERFORMING ORGANIZATION REPORT NUMBER
Naval Surface Warfare Center, Dahlgren Division Dahlgren, VA 22448	

9. SPONSORING/MONITORING AGENCY NAME(S) AND ADDRESS(ES)	10. SPONSOR/MONITOR'S ACRONYM(S)
	11. SPONSOR/MONITOR'S REPORT NUMBER(S)

12. DISTRIBUTION/AVAILABILITY STATEMENT
Approved for public release, distribution unlimited

13. SUPPLEMENTARY NOTES

See also ADM002371. 2013 IEEE Pulsed Power Conference, Digest of Technical Papers 1976-2013, and Abstracts of the 2013 IEEE International Conference on Plasma Science. Held in San Francisco, CA on 16-21 June 2013. U.S. Government or Federal Purpose Rights License.

14. ABSTRACT

When pulse-generating circuits excite antennas, the antenna often plays a major role in determining the characteristics of the radiated signal. Defining an equivalent electrical circuit for the antenna allows the simulation of the antennas transient behavior. This type of simulation, carried out with circuit analysis software, generates time-domain currents at different points on the antenna structure. From these currents, the time-domain radiated electric field can be calculated. This paper describes a procedure for developing a distributed RLC circuit model for a monopole antenna above a ground plane. The results from the modeling are compared to measurements of antenna current and radiated electric field.

15. SUBJECT TERMS

16. SECURITY CLASSIFICATION OF:			17. LIMITATION OF ABSTRACT	18. NUMBER OF PAGES	19a. NAME OF RESPONSIBLE PERSON
a. REPORT **unclassified**	b. ABSTRACT **unclassified**	c. THIS PAGE **unclassified**	**SAR**	**4**	

Fig. 2 shows a 10-stage circuit model for the monopole antenna in Fig. 1, and lists the circuit element values obtained using the procedures described above.
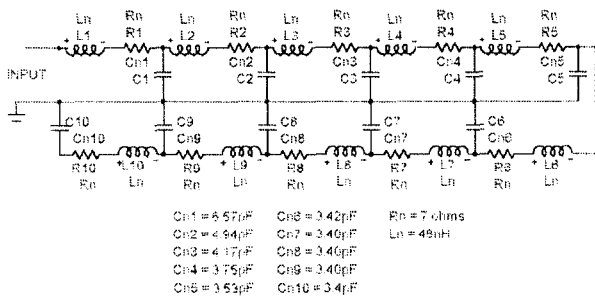

Figure 2. Monopole antenna circuit model

III. TEST SETUP

A test setup was designed to measure the antenna transient behavior. A high-voltage step transition was applied to the antenna input, and the resulting input current, tube surface currents, and radiated electric and magnetic fields were measured.

The antenna tube was positioned vertically over a brass-screen ground plane that is housed in a 12.2-m wide, 30.5-m long metal-skin building. Two dielectric angled braces keep the tube vertical. The base of the tube is separated from the ground plane by a small spark gap and a current-viewing resistor (CVR), as shown in Fig. 3. One spark gap electrode is connected to ground plane and the other is connected to the tube base through a coaxial CVR (T&M Research SBNC-1-05). During operation, the tube is charged to 17.5 kV, with respect to the ground plane, by a resistively isolated power supply. When the spark gap breaks-down, the desired voltage transition is generated. The spark gap operated in a stable, repetitive, self-breakdown mode with a gap spacing of 1.9 mm, and at an operating pressure of 2 atm (30 psi).
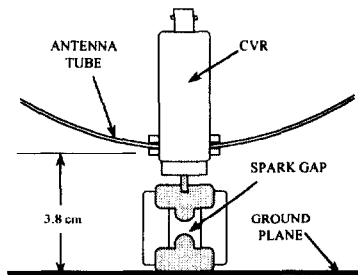

Figure 3. View of antenna input region.

A. Circuit Model

To represent the test circuit, the antenna circuit requires the addition of a spark-gap model. The spark gap is modeled as the series combination of an ideal switch, a 1-

Ω resistor, and a 50-nH inductor. These elements are connected across the input terminals of the antenna circuit. All of the capacitors in the circuit are initially charged to 17.5 kV, the measured breakdown voltage. A transient analysis of the model was performed using Micro-Cap-V circuit analysis software. Fig. 4 shows the calculated distributed currents on the ten antenna sections. Start-time and relative amplitude distinguishes the different stage currents. The transient current appears first at the input followed by each subsequent stage current. The current amplitude also progressively decreases with stage distance from the input.
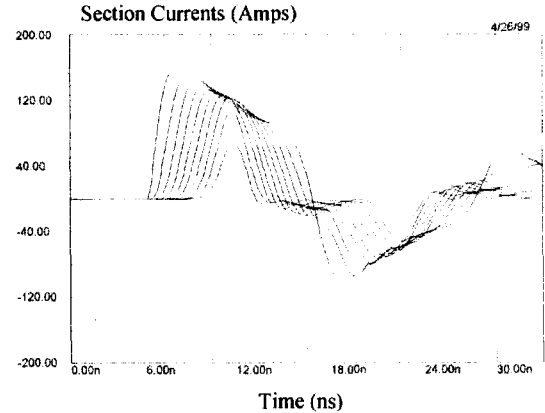

Figure 4. Calculated antenna distributed currents.

IV. RADIATION MODEL

Radiated electric field is the result of charge acceleration on the antenna structure. With certain assumptions, charge acceleration can be equated to the time-derivative of the current. This approach was used to derive the following equation for the radiated (far field) electric field due to a current flowing in an electrically short conductor.

$$E_\theta = \frac{l}{4\pi\varepsilon\,c^2 R}\frac{dI}{dt}\sin\theta \qquad (V/m) \qquad (1)$$

This equation is specified in spherical coordinates. The current, I, flows in the z direction, R is the distance from the conductor-center to the field calculation point, l is the length of the conductor, c is the speed of light, ε is the permitivity of free space, and θ is the angle between the I and R vectors (referenced to the z axis). This equation was derived from the theory of radiation due to an accelerating point charge [2], with the assumptions that the risetime of the transient current is long compared to the propagation-time across the conductor, and that $R >> l$.

The monopole radiation model treats each of the antenna's ten sections as a radiating element obeying Eq. 1. The element currents are the circuit model currents. The radiated electric field at any point is the vector sum of the contribution from each current element, taking into account the appropriate propagation delays

261

between each element and the field calculation point. An image monopole-tube below the ground plane simulates the contributions of ground-plane reflections to the radiated field.

Figure 5 shows the calculated, vertically polarized, electric field at two different points in space. These points are defined by a 10-m range (measured from the input) and elevation angles (referenced from the ground plane) of 0 and 60 degrees. These waveforms illustrate that both the peak amplitude and waveform shape change as a function of location.
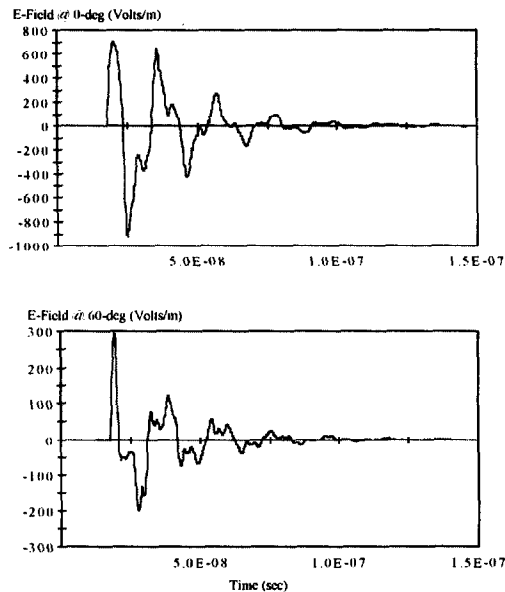
E-Field @ 0-deg (Volts/m)

E-Field @ 60-deg (Volts/m)

Time (sec)

Figure 5. Calculated electric field at two points in space: (top) 10-m range, 0-degrees elevation; (bottom) 10-m range, 60-degrees elevation

V. MEASUREMENTS AND ANALYSIS

Five different measurements were made during the antenna characterization tests: (1) antenna input current, (2) tube surface current, (3) radiated electric field, (4) radiated magnetic field, and (5) charging voltage. All sensors were electrically isolated by fiber-optic links from the recording instrument, a LeCroy LC574A digital oscilloscope, located in a shielded enclosure. Each of the above measurements, with the exception of the voltage, will be addressed separately in the following subsections. A Tektronics P6015 high-voltage probe measures the antenna charge voltage prior to the spark-gap switch turning on. This value is used as an initial condition in the circuit model. This signal is transmitted to the oscilloscope through a 10-MHz-bandwith fiber optic link (Ross VDB 50-10).

A. Input Current

The input current was measured by the 0.05-Ω CVR that is illustrated in Fig. 3. A high-bandwidth fiber-optic link (Nanofast OP 300-2A) transmits the signal to the oscilloscope. The bandwidth of this measurement system is 1-GHz. Fig. 6 shows the measured input current superimposed on the circuit-model prediction. The measured waveform is an average of 100 pulses. The initial 10-to-90-% risetime is approximately 2 ns, and the period of the oscillations is approximately 20 ns. The risetime is mainly controlled by the spark-gap turn-on time, and the period is related to the four-way transient time of the induced voltage transient between the antenna input and the end of the tube. The decay in current amplitude during the first half cycle is caused by the increase in antenna impedance with distance from the input. A resurgence in the decaying signal amplitude (~75 ns from the beginning of the waveform) is consistent with a reflection from the building end-walls, the closer one being 11 m from the antenna. However, no obvious signs of reflections are observed coming from the much-closer side walls. This is the result of the antenna being centered between these walls, and the magnetic components of the two reflected EM-fields canceling when they arrive back at the antenna.
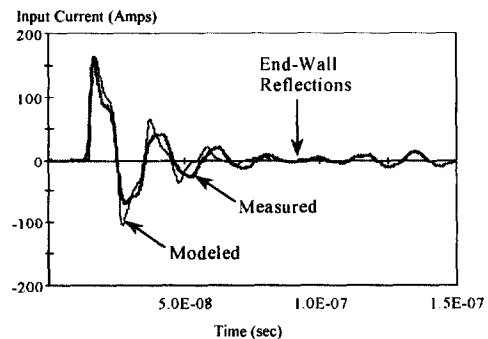
Figure 6. Antenna input current, comparison of measured to modeled waveforms.

Comparison of the measured and modeled currents in Fig. 6 show good general agreement in amplitude and ringing frequency. The model, however, predicts a faster initial risetime and higher overshoot in the leading edges of the second and subsequent half-cycles. This difference may, in part, be due to the spark-gap circuit model not accounting for the time-varying arc resistance that increase near the current zero crossings.

B. Surface Currents

The surface currents were measured at nine equally spaced points along the length of the antenna tube. These currents were obtained indirectly by measuring the derivative of the magnetic flux density (B-dot) on the

262

surface of the tube. An EG&G (MGL-S7D(R)) B-dot sensor was used to measure the field. From Amperes Law and because of symmetry, the current is the product of the measure magnetic field and the circumference of the tube. The same fiber-optic link was used as in the CVR measurement, but in this case a built-in active integrator was added to convert B-dot to B. The 1µs integrator limits the bandwidth of the measurement to approximately 300 MHz.

Fig. 7 shows the nine measured surface currents along with the measured input (CVR) current, included for comparison. These surface currents show the same general behavior as the modeled currents in Fig. 4. The peak amplitudes of the measurements are approximately 20% lower.
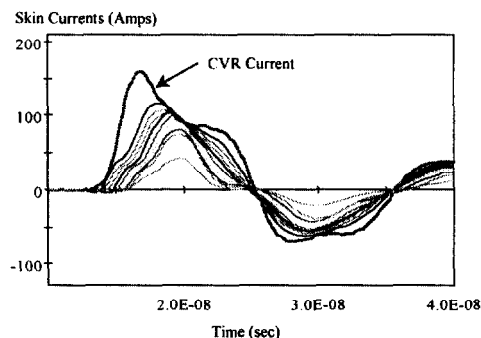

Figure 7. Measured monopole surface currents and input (CVR) current.

C. *Radiated Fields*

Electric and magnetic fields in the vicinity of the monopole were measured using D-dot and B-dot probes (EG&G ACD-4C(R) and MGL-2D(A) respectively) and the same integrating fiber-opting link used in the skin current measurements. Fields measured at 4 m (horizontal distance) from the antenna tube and 1.27 m above the ground plane (centered between the side walls) were selected for comparison to the modeled results. At this point in space the ratio of the measured orthogonal electric and magnetic fields equals, within a few percent, the impedance of free space, indicating the presence of a radiated electromagnetic wave. However, a limited time window of approximately 30 ns exists before the arrival of wall reflections. Unlike the magnetic-field, the reflected electric fields arrive in-phase at the center and reinforce each other. Fig. 8 shows a comparison between the measured and modeled electric field. There is good agreement between the measured and modeled waveforms before the arrival of reflections. The main differences are higher amplitude on the first peak and an overshoot in the beginning of the second and third half-cycles in the modeled results. Risetime and amplitude differences

between the measured and modeled currents account for part of these differences in the measured and modeled fields.
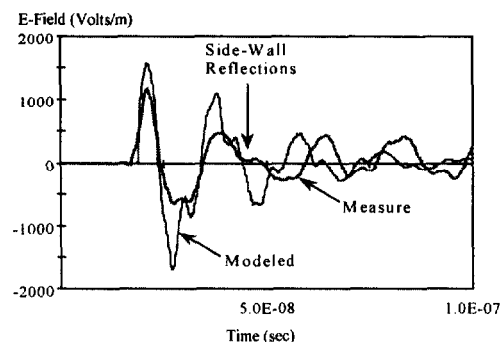

Figure 8. Comparison of modeled and measured electric field at a 4.2-m range and 17.6-degree elevation.

VI. CONCLUSIONS

The reported results show that a distributed-element circuit model is a valid way to represent an antenna's transient behavior. Also demonstrated, was a transient radiation model based on the calculated antenna currents and a derived equation for the radiated field.

For model verification, a relatively simple circuit that generated a stepped-voltage was used to excite the antenna model; however, a model of this type can be driven by very complex circuits as long as they can be modeled with circuit analysis software.

Although developed in this case for a monopole antenna, this model can be applied to other similar types of antennas. The main requirement is identifying the propagation volume of the antenna and the associated distributed capacitance and inductance. A distributed resistance must also be included that is presently experimentally determined. Finding an analytical method of obtaining this resistance is a potential area of improvement for the antenna model.

VII. REFERENCES

[1] H. Knoepfel, *Pulsed High Magnetic Fields*. New York; American Elsevier Publishing Co., 1970, p313.

[2] J. D. Jackson, *Classical Electrodynamics*. New York: John Wiley & Sons, 1962, p 468.

263